Core-crosslinked micelles with a poly-anionic poly(styrene sulfonate)-based outer shell made by RAFT polymerization

Hui Wang, Christophe Fliedel, Eric Manoury, Rinaldo Poli

Core-crosslinked micelles with a poly-anionic poly(styrene sulfonate)-based outer shell made by RAFT polymerization

Hui Wang,[†] Christophe Fliedel[†], Eric Manoury[†], Rinaldo Poli[†‡]*

[†] *LCC (Laboratoire de Chimie de Coordination), Université de Toulouse, CNRS, UPS, INPT, 205 route de Narbonne, BP 44099, F-31077 Toulouse Cedex 4, France CNRS. Fax: +33-561553003; Tel: +33-561333174; E-mail:rinaldo.poli@lcc-toulouse.fr.*

[‡] *Institut Universitaire de France, 1, rue Descartes, 75231 Paris Cedex 05, France.*

KEYWORDS

Core-crosslinked micelles; Poly(styrene sulfonate); RAFT polymerization; Polymerization-induced self-assembly

Abstract

Core-crosslinked micelles (CCMs) with a permanently charged anionic shell of sodium poly(styrene sulfonate) (PSS^-Na^+) chains have been developed by a convergent three-step one-pot RAFT polymerization starting with 4-cyano-4-thiothiopropylsulfanyl pentanoic acid (CTPPA, R_0-SC(S)S*n*Pr) as chain transfer agent, which includes polymerization-induced self-assembly (PISA) in the second step. The final crosslinking step of the R_0-$(SS^-Na^+)_x$-*b*-St_y-SC(S)S*n*Pr diblock chains was carried out with diethylene glycol dimethacrylate (DEGDMA), either diluted into styrene (DEGDMA/St = 10:90) or neat. The morphology of the intermediate micelles and of the final CCM particles was studied by dynamic light scattering (DLS) and transmission electron microscopy (TEM) as a function of the relative degrees of polymerizations for the shell, core, and crosslinking blocks. Conformational instability was observed for the aqueous dispersions of the diblock micelles, especially with the shorter PSt blocks, yielding equilibria with single chains and large agglomerates. However, crosslinking led to well-defined CCMs with narrow size distributions for the optimized polymer compositions. The DLS analysis in a compatibilizing 60:40 THF/H_2O solvent mixture demonstrates that the final step of the polymer synthesis has quantitatively crosslinked all diblock arms.

1. Introduction

Unimolecular (crosslinked) micelles are attracting growing attention for multiple applications such as drug delivery, light harvesting, tissue engineering and as nanoreactors for catalysis. By far, the most useful micelles are those with a hydrophilic outer shell and a hydrophobic core for confinement in aqueous media. The development of this area of polymer synthesis has greatly been stimulated by recent progress in living/controlled polymerization techniques, particularly controlled radical polymerization, which have allowed the synthesis of tailored functionalized amphiphilic block copolymers capable of spontaneous self-assembly. Crosslinking, which may be realized either on the shell, in the core, or at an intermediate corona level for multiblock copolymer micelles, removes the

dynamic equilibrium between the micellar objects and the free arm constituents, thus improving properties such as drug loading capacity, stability, and confinement in the aqueous medium.[1-8]

Controlled radical polymerizations are compatible with water as reaction medium, in addition to being applicable to a wide range of monomers and can be implemented under less stringent conditions relative to the non-radical methods. Among the various possible techniques, reversible addition-fragmentation chain-transfer (RAFT) polymerization has been very successful,[9, 10] particularly when combined with "polymerization-induced self-assembly" (PISA),[11-15] directly leading to crosslinked particles in a one-pot process in water.[16-23] In our laboratory, we have focused on core-crosslinked micelles (CCM), which are accessible by a simple a 3-step convergent synthesis. In the first step, a water-soluble monomer (or comonomer mixture) is polymerized with a chain transfer agent R_0-SC(S)Z in water (solution polymerization) to yield a hydrosoluble macroRAFT agent R_0-P^1-SC(S)Z where P^1 is a first (co)polymer block. This is followed in a second step by a dispersion polymerization of a hydrophobic monomer or comonomer mixture, which turns into an emulsion polymerization after self-assembly, to generate micelles of the amphiphilic R_0-P^1-*b*-P^2-SC(S)Z diblock copolymer macroRAFT agent. The third and final step consists of the RAFT polymerization of a lipophilic bifunctional monomer, resulting in micelle core crosslinking.

In recent work, we have employed this method to develop CCM particles that are stabilized by either a neutral or a polycationic hydrophilic shell. Our first-generation CCMs, stabilized by a neutral outer block,[24] were assembled starting from a tricarbonate chain transfer agent R_0-SC(S)Z (4-cyano-4-thiothiopropylsulfanyl pentanoic acid or CTPPA, where Z = S*n*Pr and R_0 = C(Me)(CN)-CH_2CH_2COOH) by the random copolymerization of methacrylic acid (MMA) and poly(ethylene oxide) methacrylate (PEOMA). These CCMs contain a differently functionalized polystyrene core,[24-26] assembled by the copolymerization of styrene and a phosphine-functionalized styrene monomer. The final crosslinking step was achieved with a 90:10 mixture of styrene and diethyleneglycol dimethacrylate (DEGDMA), with formation of a central P(St-*co*-DEGDMA) nanogel core. The high dilution of the DEGDMA crosslinker with styrene was needed to avoid macrogelation, which is

caused by reversible micelle interpenetration during the cross-linking reaction. The optimized chain composition for good control of the spherical morphology and of the size distribution is R_0-(MAA$_{0.5}$-*co*-PEOMA$_{0.5}$)$_{30}$-*b*-(FS$_x$-*co*-St$_{1-x}$)$_{300}$-*b*-(DEGDMA$_{0.1}$-*co*-St$_{0.9}$)$_{100}$-SC(S)S*n*Pr (FS = functionalized styrene, *e.g.* diphenylphosphinostyrene; x = variable fraction, note that we use the abbreviation St for styrene in this contribution, to avoid confusion with the sulfur atom of the RAFT agent). These CCMs were loaded with metal complexes by coordination to the functionalized monomers in the core and applied as catalytic nanoreactors under aqueous biphasic conditions.[24-31]

Because of decantation speed and catalyst leaching issues, we have subsequently developed second-generation CCMs, which differ from the first-generation CCMs in the hydrophilic shell composition: the neutral P(MAA-*co*-PEOMA) block was replaced by a P(VPMe$^+$I$^-$) block, where VPMe$^+$I$^-$ = *N*-methyl-4-vinylpyridinium iodide). In this case, the optimized composition of the diblock intermediate for morphology and size control is R_0-(VPMe$^+$I$^-$)$_{140}$-*b*-(FS$_x$-*co*-St$_{1-x}$)$_{300}$-SC(S)S*n*Pr.[32, 33] A first optimization study carried out in the absence of FS (x = 0) revealed that the final crosslinking step was also quite efficient when using neat DEGDMA thanks to the Coulombic shell-shell repulsion, which blocks particle interpenetration.[32] However, the successful diblock copolymer assembly required two additional steps, a solvent change and the isolation of an intermediate. This results from the failure of the VPMe$^+$I$^-$ monomer to polymerize under the RAFT conditions in water and from the failure to chain-extend an indirectly generated hydrophilic R_0-(VPMe$^+$I$^-$)$_{140}$-SC(S)S*n*Pr macroRAFT agent with styrene. The successful synthesis required an initial RAFT polymerization of vinyl pyridine (VP), followed by chain extension with a short (50 units) polystyrene block and quaternization of the PVP block monomers with MeI. Subsequently, further chain extension with a longer PS block and final crosslinking successfully completed the synthesis. This strategy was then extended to the generation of phosphine-functionalized CCMs for catalytic applications, pleasingly yielding improved performances (faster decantation and lower catalyst leaching).[33, 34]

Micelles with polyanionic shells are less frequent than their polycationic and neutral counterparts. Examples are the diblock copolymer micelles containing P(SPMA$^-$K$^+$),[35] P(SPMA$^-$K$^+$-*co*-HEMA),[35] PSS$^-$Na$^+$[36, 37] and PAMPS$^-$Na$^+$[38] outer shells (SPMA$^-$K$^+$ = potassium 3-sulfopropyl methacrylate; HEMA = hydroxyethyl methacrylate; SS$^-$Na$^+$ = sodium 4-vinylbenzenesulfonate or *p*-styrenesulfonate; AMPS$^-$Na$^+$ = sodium 2-acrylamido-2-methylpropane sulfonate). However, no example of unimolecular (crosslinked) micelles with a permanent polyanionic shell has so far been reported to the best of our knowledge. Anionic-shell CCMs have previously been obtained only by deprotonation of carboxylic acid groups from neutral-shell CCMs at high pH, *e.g.* by deprotonating the MAA monomers in our first generation CCMs.[39, 40] We report here the synthesis and characterization of CCMs with a permanent polyanionic shell and a non-functionalized polystyrene core. The development of equivalent phosphine-functionalized particles and their application as catalytic nanoreactors will be the topic of a separate contribution.

2. Experimental

2.1. Materials and methods.

All manipulations were performed by Schlenk-line techniques under an inert atmosphere of dry argon. Solvents were dried by standard procedures and distilled under argon prior to use. 4,4'-azobis(4-cyanopentanoic acid) (ACPA, >98%, Fluka), sodium 4-vinylbenzenesulfonate (SS$^-$Na$^+$, >90%, Aldrich), diethylene glycol dimethacrylate (DEGDMA, 95%, Aldrich), and 1,3,5-trioxane (>99%, Aldrich), were used as received. Styrene (St, 99%, Acros) was distilled under reduced pressure prior to use. The RAFT agent 4-cyano-4-thiothiopropylsulfanyl pentanoic acid (CTPPA) or R_0-SC(S)S*n*Pr (R_0 = -C(CH_3)(CN)CH_2CH_2COOH), was prepared according to the previously described method.[41] The deionized water used for the syntheses and DLS analyses was obtained from a Purelab Classic UV system (Elga Lab-Water).

2.2. Characterization Techniques.

NMR spectroscopy. All nuclear magnetic resonance spectra were recorded in 5 mm diameter tubes at 297 K on a Bruker Avance 400 spectrometer. The ^{1}H chemical shift was determined using the residual peak of the deuterated solvent (δ 2.50 for DMSO-d_6, 4.79 for D_2O) as internal standard and are reported in ppm (δ) relative to tetramethylsilane. The monomer conversions in the polymerizations were monitored by ^{1}H NMR in DMSO-d_6 at room temperature by the relative integration of the protons of the internal reference (1,3,5-trioxane) at 5.20 ppm and the vinylic monomer protons.

Size exclusion chromatography (SEC). The P(SS^-Na^+) chain growth was monitored by SEC in water/acetonitrile (80:20 v/v) with 0.1 M $NaNO_3$ at 60 °C at a flow rate of 1.0 mL min^{-1} by using a Viscotek TDA305 apparatus (SEC-DMF) coupled with a multi-angle light scattering (MALLS) detector (18 angles). The measured d*n*/d*c* values for the R_0-$(SS^-Na^+)_{140}$-SC(S)S*n*Pr in the eluent is 0.199 mL g^{-1}. All polymers were analyzed at a concentration of 5 mg mL^{-1} after filtration through 0.45 μm pore size membrane. The separation was carried out on 2 columns Agilent Aquagel OH Mixed M. The software used for data collection and calculation was OmniSec version 4.7 from Malvern Instruments.

Dynamic light scattering (DLS). The intensity-average diameters of the latex particles (D_z) and the polydispersity index (PDI) were obtained on a Malvern Zetasizer NanoZS equipped with a He-Ne laser (λ = 633 nm), operating at 25 °C. Samples were analyzed after dilution (0.05 ml latex with 1 ml of deionized water) either unfiltered or after filtration through a 0.45 μm pore-size membrane. The procedure without filtration allowed verification of the presence of agglomerates. Zeta potential (ζ) determinations were also conducted on the same instrument by measuring the electrophoretic mobility.

Transmission electron microscopy (TEM). The morphological analyses of the copolymer nano-objects were performed at the Centre de Microcaractérisation Raimond Castaing (Toulouse France) with a JEOL JEM 1400 transmission electron microscope working at 120 kV. One drop of the diluted and unfiltered latex samples (obtained by adding 3 drops of the synthesized latexes in 2 mL of distilled

water) was dropped on a formvar/carbon-coated copper grid and dried under vacuum for 24 hours. The sample were not stained.

2.3. Preparation of a latex of a P(SS$^-$Na$^+$)-*b*-PSt amphiphilic block copolymer.

A stock solution of water ACPA/$NaHCO_3$ was prepared with 5 mL of H_2O and dissolution of ACPA/$NaHCO_3$ (0.10 g / 0.10 g), [ACPA] = 71.4 mmol L^{-1}.

Step 1: Preparation of R_0-(SS$^-$Na$^+$)$_x$-SC(S)SnPr. A. x = 140. A portion of the ACPA stock solution (1 mL, 20 mg of ACPA, 0.071 mmol), CTPPA (0.1 g, 0.36 mmol), SS$^-$Na$^+$ (10.42 g, 50.54 mmol; SS$^-$Na$^+$/CTPPA = 140), ethanol (27 mL) and deionized water (63 mL) were added to a 250 mL Schlenk tube with a magnetic stirrer bar. An internal reference (1,3,5-trioxane, 0.16 g, 1.84 mmol) was also added as for the determination of the monomer conversion as a function of time by ^{1}H NMR. The solution was purged for 45 min with argon and then heated to 80 °C during 20 h in a thermostatic oil bath under stirring, leading to nearly quantitative monomer conversion (residual unreacted styrene estimated as < 1% by ^{1}H NMR, see SI). The experimental molar mass (from SEC) for the final polymer is M_n = 24400 g mol^{-1} with $Đ$ = 1.04, versus a theoretical molar mass of 29100 g mol^{-1}. The polymer content in the latex is 10.98 % w/w.

B. x = 50. This procedure is identical to that described above, using 1 mL ACPA stock solution (20 mg of ACPA, 0.071 mmol), CTPPA (0.1 g, 0.36 mmol), SS$^-$Na$^+$ (3.72 g, 18.05 mmol; SS$^-$Na$^+$/CTPPA = 50), ethanol (13.5 mL), deionized water (31.5 mL) and 1,3,5-trioxane (59.6 mg, 0.66 mmol). The experimental molar mass (from SEC) for the final polymer is M_n = 19680 g mol^{-1} with $Đ$ = 1.17, versus a theoretical molar mass of 10604 g mol^{-1}. The polymer content in the latex is 8.10 % w/w.

Step 2. MacroRAFT chain extension with styrene. Preparation of R_0-(SS$^-$Na$^+$)$_x$-b-St$_y$-SC(S)SnPr.

This procedure is described in detail only for x = 140, y = 300. In a 100 mL Schlenk tube, 10 mL R_0-(SS$^-$Na$^+$)$_{140}$-SC(S)S*n*Pr latex obtained in the previous step (0.04 mmol of polymer, corresponding to 5.46 mmol of SS$^-$Na$^+$ units) were diluted with 3 mL H_2O. To this solution was added degassed styrene (1.346 mL, 1.219 g, 11.70 mmol, 300 equiv. per chain) slowly *via* syringe. Then a

degassed ACPA/$NaHCO_3$ stock solution (0.11 mL, 2.2 mg ACPA, 7.99 µmol) was added and the resulting reaction mixture was stirred at 80 °C for 4 h. The styrene consumption was complete and was accompanied by the transformation of the initial suspension into a stable latex of R_0-(SS^-Na^+)$_{140}$-*b*-St_{300}-SC(S)S*n*Pr macromolecules, self-assembled in the form of micelles to yield a light yellow opalescent stable dispersion (DLS: D_z = 91.8 nm; PDI = 0.41, filtered through a 0.45 µm pore filter). The molar mass calculated for R_0-(SS^-Na^+)$_{140}$-*b*-St_{300}-SC(S)S*n*Pr is 60360 g mol^{-1}. The polymer content in the latex is 16.1 % w/w.

2.4. Cross-linking of the PSS^-Na^+-*b*-PS amphiphilic block copolymer by DEGDMA.

(a) In the presence of styrene. Preparation of R_0-(SS^-Na^+)$_{140}$-b-St_{300}-b-($S_{0.9}$-co-$DEGDMA_{0.1}$)$_{150}$-SC(S)SnPr. To the total amount of the R_0-(SS^-Na^+)$_{140}$-*b*-St_{300}-SC(S)S*n*Pr latex obtained in step 2 (0.04 mmol of polymer) were successively added 3 mL H_2O, degassed styrene (0.606 mL, 0.549 g, 5.27 mmol, 135 equiv. per chain), DEGDMA (0.131 mL, 141.6 mg, 0.59 mmol, 15 equiv. per chain), and a degassed ACPA/$NaHCO_3$ stock solution (0.11 mL, 2.2 mg of ACPA, 7.99 µmol). The resulting reaction mixture was stirred at 80 °C for 2 h resulting in an essentially quantitative monomer consumption (< 1% of residual styrene by ^{1}H NMR monitoring in DMSO-d_6) to yield R_0-(SS^-Na^+)$_{140}$-*b*-St_{300}-*b*-($S_{0.9}$-*co*-$DEGDMA_{0.1}$)$_{150}$-SC(S)S*n*Pr. The polymer content in the latex is 16.4 % w/w. The calculated for molar mass per chain is 78070 g mol^{-1}.

(b) With neat DEGDMA. Preparation of R_0-(SS^-Na^+)$_{140}$-b-St_{300}-b-$DEGDMA_{15}$-SC(S)SnPr. To the total volume of the R_0-$SS^-Na^+_{140}$-*b*-St_{300}-SC(S)S*n*Pr latex obtained in step 2 (0.04 mmol of polymer) were successively added 3 mL of H_2O, DEGDMA (0.131 mL, 141.6 mg, 0.59 mmol, 15 equiv. per chain) and the degassed ACPA/$NaHCO_3$ stock solution (0.11 mL, 2.2 mg ACPA, 7.99 µmol). The resulting reaction mixture was stirred at 80 °C for 2 h resulting in an essentially quantitative monomer consumption (< 1% of residual DEGDMA by ^{1}H NMR monitoring in DMSO-d_6) to yield R_0-$SS^-Na^+_{140}$-*b*-St_{300}-*b*-$DEGDMA_{15}$-SC(S)S*n*Pr. The polymer content in the latex is 13.8 % w/w. The calculated for molar mass per chain is 63990 g mol^{-1}.

2.5. Preparation of R_0-St_{300}-SC(S)S*n*Pr

A 0.2 mL portion of an ACPA stock solution, prepared with ACPA/$NaHCO_3$ (0.10 g / 0.10 g) in 5 mL of H_2O (4 mg of ACPA, 0.014 mmol), CTPPA (20.1 mg, 72.56 µmol), styrene (2.26 g, 21.7 mmol; S/CTPPA = 300) and DMF (5 mL) were added to a 50 mL Schlenk tube with a magnetic stirrer bar. An internal reference (1,3,5-trioxane, 19.5 mg, 0.22 mmol) was also added as for the determination of the monomer conversion as a function of time by ^{1}H NMR. The solution was purged for 45 min with argon and then heated to 80 °C during 5 h in a thermostatic oil bath under stirring, leading to nearly quantitative monomer conversion (the residual unreacted styrene was estimated as 12.2 % by ^{1}H NMR).

3. Results and Discussion

The polymer synthesis, summarized in Scheme 1, followed the same procedure that was previously adopted for the first-generation CCM particles with a neutral hydrophilic P(MAA-*co*-PEOMA) shell.[24] For convenience, all polymers reported in this contribution and reference to their characterization data are collected in Table S1.

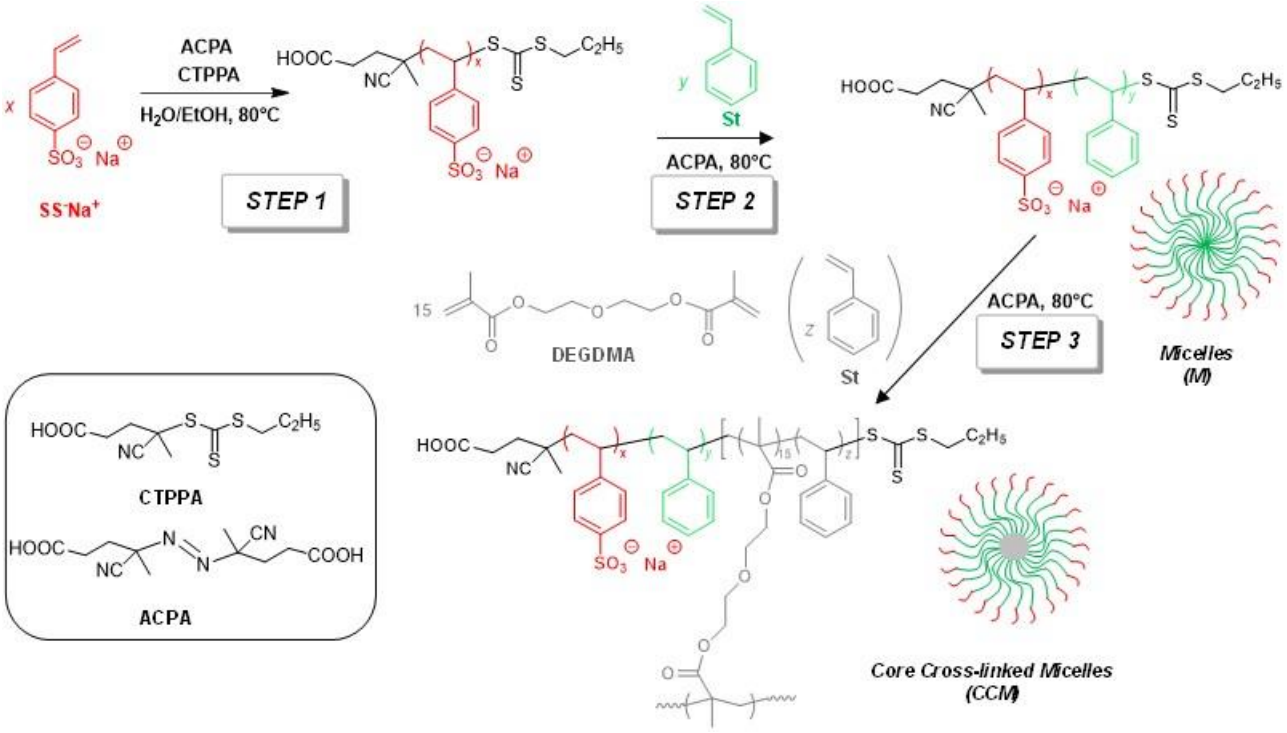

Scheme 1. Synthetic scheme for the core-crosslinked micelles containing a polyanionic P(SS^-Na^+)-based shell.

3.1. P(SS$^-$Na$^+$) macroRAFT

The first step, consisting of the SS$^-$Na$^+$ RAFT polymerization in a water/ethanol (70:30 v/v) mixture, proceeded to complete conversion (see SI, Figure S1) with good control (low-dispersities and target molar masses, Figure S2) to yield the macroRAFT agents R_0-(SS$^-$Na$^+$)$_x$-SC(S)S*n*Pr, where the chain ends derive from the CTPPA RAFT agent. Two quite different target degrees of polymerization (x = 50 and 140) were used to assess the stability of the final CCM particles with respect to this parameter. The DLS and TEM characterization of the macroRAFT products is available in Figure S3. The DLS of the polymer aqueous solutions shows narrow distributions of small objects (average diameter ~ 1 nm), probably corresponding to solvated single chains, though a small contribution of large agglomerates (d ~ 300 nm) is also present but visible only in the intensity mode. The TEM analysis of the solid residue shows only large agglomerates.

3.2. P(SS$^-$Na$^+$)-*b*-PSt diblock macroRAFT

The chain extension of P(SS$^-$Na$^+$) macroRAFT agents with a polystyrene block in water has previously been described,[42-45] as was also the chain extension with other monomers (vinylidene chloride[36] and acrylates[36, 37]). Chain extensions with PISA in water have also been reported for other anionic macromonomers.[46-49] A P(SS$^-$Na$^+$)-*b*-PSt diblock copolymer had also been indirectly obtained by extending a hydrophobic P(SS$^-$Oct$_3$NH$^+$) macroRAFT agent with styrene in benzene or chlorobenzene, followed by trioctylammonium/sodium exchange,[50] as well as by chain extension of a P(SS$^-$Na$^+$)-TEMPO macroinitiator with styrene by nitroxide-mediated polymerization (NMP).[51] The chain extension of both R_0-(SS$^-$Na$^+$)$_x$-SC(S)S*n*Pr macroRAFT agents (x = 50 and 140) with styrene proceeded without difficulty. This step entails polymerization-induced self-assembly (PISA) and proceeds up to essentially quantitative styrene conversion (see Figure S4) and with good control (molar masses linearly growing with conversion, low Đ, see Table S2 and Figure S5) to afford translucent dispersions (see Figure S6), indicating successful micellization. The DLS and TEM

characterization of the resulting diblock macroRAFT latexes revealed interesting phenomena. Chain extension of the short (x = 50) P(SS^-Na^+) chain with a long (y = 300) PSt block yielded a relatively large number of particles narrowly distributed around d ~ 40 nm, but also larger aggregates (low in number but relevant in intensity) around d ~ 200 nm (Figure S7a). Chain extension of the longer (x = 140) P(SS^-Na^+) chain with a short (y = 50) PSt block yields morphologically unstable latexes. The DLS of the R_0-(SS^-Na^+)$_{140}$-*b*-St_{50}-SC(S)S*n*Pr solution shows relatively homogeneous large aggregates (d > 500 nm) for the unfiltered solution, whereas after filtration single chains (d ~ 1 nm) become the dominant distribution in number, while the TEM characterization suggests that the large objects are vesicles (Figure S7b). Extension of the same long P(SS^-Na^+) chain with a longer PSt block (y = 300, 350 or 380), however, led to more stable and more narrowly distributed small micelles (d ~ 20 nm), although a small number of larger particles are also present (Figure S7c-e).

In order to learn more about the instability witnessed for the R_0-(SS^-Na^+)$_{140}$-*b*-St_{50}-SC(S)S*n*Pr latex, a few additional DLS investigations were carried out for this polymer dispersion, in comparison with the more stable R_0-(SS^-Na^+)$_{140}$-*b*-St_{350}-SC(S)S*n*Pr polymer (Figure S8). After freeze-drying, these two polymers were dispersed again in water. The resulting DLS plots (Figure S8a) compare quite well with those of the pristine latex from synthesis after filtration, *i.e.* mostly single chains for the polymer with the short St_{50} block and a broad distribution of agglomerates for the polymer with the longer St_{350} block, although the distribution of the latter is somewhat narrower than in the pristine latex. Redispersion of the freeze-dried samples in a 60:40 THF-H_2O solvent mixture, which is the best compatibilizing medium (*vide infra*), does not dramatically change the distributions (Figure S8b), except for a further sharpening in the case of the longer PSt block sample. A most interesting phenomenon was observed immediately after the addition of a small amount of water to the THF-H_2O dispersion of the short PSt block sample (Figure S8c). Five measurements were collected at ca. 20 second intervals starting immediately after the water addition. The single chains, with diameter peaking at around 0.6 nm, evolved toward larger objects (d ca. 20 nm) after the second measurement. The same evolution (not reported in the figure) was observed for the volume and intensity

distributions. However, after the end of these measurements, the cuvette with the sample was shaken, left to stand undisturbed for 3 min and then remeasured, yielding consistent (invariable with time) distributions consisting mostly, once again, of single chains (maximum at ca. 0.6 nm for the number and volume distributions and bimodal distribution for the in the intensity mode, with the larger particles peaking at ca. 35 nm), see Figure S8d. In parallel, the R_0-$(SS^-Na^+)_{140}$-*b*-St_{350}-SC(S)S*n*Pr sample did not show any significant evolution, neither with time nor after shaking and resting. Finally, a much larger amount of water (dilution by a factor of ten) was added to the dispersions resulting from the previous measurement. Under these conditions, the shorter PSt block sample gave larger objects (d ca. 80 nm, see Figure S8e), the size distribution remaining unchanged over the time of five consecutive measurements, while the longer PSt block sample continued to display object with dimensions (d ca. 50 nm for the number distribution) close to those measured under the other conditions.

Following a reviewer's suggestion, we have also remeasured the DLS of one representative polymer in a high ionic-strength solution (0.1 M NaCl) under conditions where the molar $NaCl/SS^-Na^+$ ratio is 3.5. At the same time, the latex was also remeasured in pure water (several months after the original measurement reported in Figure S7d). The corresponding results are shown in Figure S9. The new DLS in water is quite consistent with the original one, underlining the long-term stability of this polymer dispersion, while the DLS in the NaCl solution is significantly sharper and monomodal, attesting the good control of the polymerization process.

All latexes show a relatively large and negative zeta potential (in the -40 to -60 mV range, see Table S1), similar to those of other micellar objects with a polyanionic shell.[35, 38] Given the relatively large standard deviations of the zeta potential values, no clear trend can be discerned. In conclusion, monomodal distributions for stable micelles were never obtained; equilibria between aggregated and small micelles (and even single chains in one case) are always observed. These equilibria appear rather delicate and affected by simple manipulations, e.g. filtration, suggesting metastability for certain dispersions. We are currently not able to rationalize this behavior. The degree of

polymerization of the P(SS^-Na^+) block (50 or 140) does not seem to make a large difference, whereas the micelles appear to be better stabilized by a longer PSt block. These results are similar to those previously obtained for the polycationic P($4VPMe^+I^-$) CCM particles.[32, 33] It is also worth mentioning that the colloidal dispersions of all synthesized polymers, both at their as-synthesized concentration and after dilution with water, do not show any notable sign of macroscopic change (*e.g.* agglomeration or creaming) over a time span of several months. Given that the morphology can vary during the crosslinking step (as we previously demonstrated for the polycationic-shell CCM particles),[33] both the shorter and longer P(SS^-Na^+) diblock macroRAFT chains were further investigated in the crosslinking step.

3.3. Crosslinking with a mixed DEGDMA and styrene mixture

The initial crosslinking experiments were carried out with the DEGDMA crosslinker diluted in styrene (DEGDMA:St = 10:90), *i.e.* the same comonomer mixture previously used to obtain the neutral-shell CCM particles, for a total of 150 monomers per chain. Two diblock copolymer macroRAFT agents, R_0-(SS^-Na^+)$_x$-*b*-St$_y$-SC(S)S*n*Pr (x = 140, y = 300 and 350), where crosslinked in these experiments. The monomer conversions were quantitative (see Figure S10). The obtained polymer particles have spherical morphology (Figure S11), relatively small size (main distribution in number with d ~ 30 and 70 nm for y = 300 and 350, respectively, from the DLS), and zeta values relatively similar to the those of the diblock precursors, but are contaminated by a larger size distribution.

3.4. Crosslinking with neat DEGDMA

Arguing that the anionic-shell CCM particles, like the previously developed cationic-shell analogues, should also benefit from Coulombic shell-shell repulsion, we then proceeded to test the crosslinking step with neat DEGDMA. The shell-shell repulsion should block the particle interpenetration phenomenon that leads to macrogelation, which was previously observed for the neutral-shell particles when using neat DEGDMA.[24] Indeed, in all cases, the crosslinking of R_0-(SS^-Na^+)$_x$-*b*-St$_y$-SC(S)S*n*Pr with neat DEGDMA produced stable white latexes. Four R_0-(SS^-Na^+)$_x$-*b*-St$_y$-

b-DEGDMA$_z$-SC(S)S*n*Pr CCM products where thus generated with (x,y,z) = 140,300,15 (*a*), 140,350,15 (*b*), 140,380,90 (*c*), and 50,300,15 (*d*). The monomer conversion was again quantitative in all cases, as shown by the NMR monitoring (Figure S12). The ^{1}H NMR spectra of the final latexes after dilution in DMSO-d_6 revealed only the resonances of the PSS$^-$Na$^+$ shell (aromatic *ortho* and *meta* H resonances centered at δ 7.4 and 6.4 and broad feature at δ 2-1 for the aliphatic backbone atoms), because the polystyrene core is not sufficiently well-swollen by this solvent. Warming the sample up to 120°C in the NMR probe did not significantly change the spectrum. However, the polystyrene core became visible after swelling the latex with $CDCl_3$ (see spectrum of sample (a) in Figure 1). The overlapping (*o*+*p*) resonance of the aromatic polystyrene protons are centered at δ ca. 7.0, whereas the *m* resonance, expected at δ ca. 6.5, overlaps with a PSS$^-$Na$^+$ shell resonance.

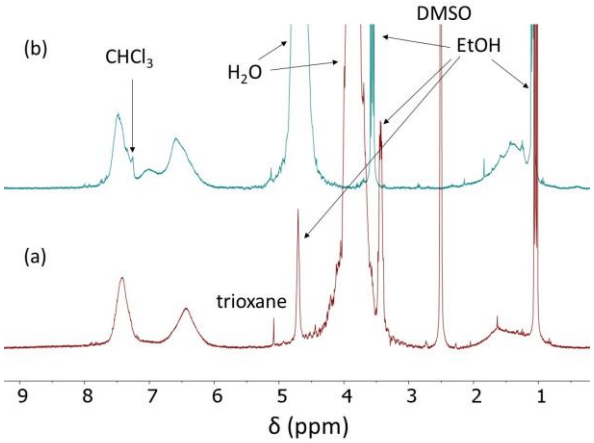

Figure 1. ^{1}H spectrum of R$_0$-(SS$^-$Na$^+$)$_{140}$-*b*-St$_{300}$-*b*-DEGDMA$_{15}$-SC(S)S*n*Pr: (a) in DMSO-d_6; (b) in D_2O after core-swelling with $CDCl_3$.

The TEM characterization of the obtained latexes confirms in all cases the presence of spherical particles of relatively small size (< 100 nm), see Figure 2. The narrow distribution of the particle size is again confirmed by the DLS analysis (Figure S13). However, a population of larger aggregates (d ~ 350 nm), small in the number distribution but dominant in the intensity distribution, was again visible for the sample *a* with y = 300 (Figure S13a). This second population was no longer observed in samples *b* (Figure S13b) and *c* (Figure S13c), for which the size distributions were quite narrow (D_z = 106 nm, PDI = 0.08; and D_z = 105 nm, PDI = 0.11; respectively). Crosslinking of the diblock macroRAFT arms with the shorter PSS$^-$Na$^+$ block (sample *d*) yielded again a minor larger size

population (ca. 100 nm in diameter, significant only in the intensity distribution), but the major population was rather narrowly distributed and with a smaller average diameter than the longer-block outer shell particles *b* and *c* (D_z = 41 nm, PDI = 0.23; Figure S13d). Therefore, even though the R_0-(SS^-Na^+)$_{50}$-*b*-St$_{300}$-SC(S)S*n*Pr diblock macroRAFT agent has a rather heterogeneous (bimodal) size distribution for the self-assembled micelles (Figure S7a), the crosslinker addition has the effect of breaking up the larger agglomerates during the crosslinking step. This reorganization phenomenon was previously observed for the equivalent polymers with a polycationic shell.[32, 33] In that case, the reorganization was attributed to a better stabilization of the spherical micelles after addition of the crosslinking monomer mixture, which was supported by DLS measurements of the swollen latex prior to the crosslinking reaction.

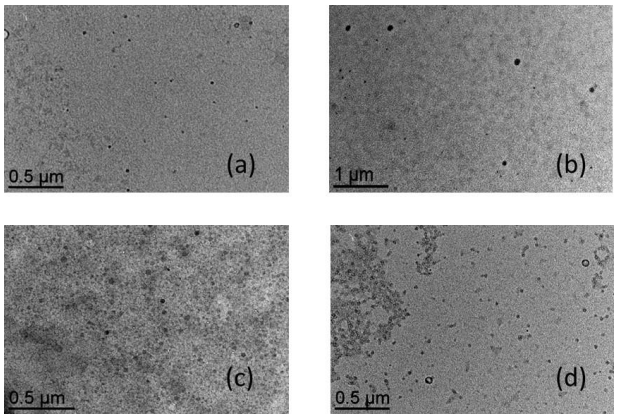

Figure 2. TEM images for the R_0-(SS^-Na^+)$_x$-*b*-St$_y$-*b*-DEGDMA$_z$-SC(S)S*n*Pr CCMs: (a) x = 140, y = 300, z = 15; (b) x = 140, y = 350, z = 15; (c) x = 140, y = 380, z = 90; (d) x = 50, y = 300, z = 15.

Additional information was sought from a DLS measurement of the R_0-(SS^-Na^+)$_{50}$-*b*-St$_{300}$-SC(S)S*n*Pr dispersion in the presence of 15 equiv. per chain of DEGDMA before the crosslinking step. This shows that, in the present case, the crosslinker addition yields a distribution dominated by a population with very small diameter (d ~ 0.6 nm, see Figure S14), consisting of single chains. Thus, the aqueous dispersion of the P(SS^-Na^+)-*b*-PSt diblock copolymers appears rather unstable, with facile equilibria that respond to minor perturbations (filtration for Figure S7b; addition of DEGDMA for Figure S14) between single chains, single spherical micelles, and larger agglomerates. In most cases, however, the CCMs with spherical morphology are the dominant product obtained from the

crosslinking step. It seems, therefore, that the combination of the crosslinking reaction and the agglomerate/micelle/single chain equilibrium dynamics has a beneficial effect in optimizing the formation of narrowly dispersed spherical particles.

It is to be noted that a quite different amount of the DEGDMA crosslinker was used for samples *b* and *c* (15 and 90 equivalents per chain, respectively). However, this difference affected neither the crosslinking efficiency nor the particle average size. The equivalence of the particle size may tentatively be attributed to a different aggregation number (greater number of chains for the CCMs with the lower DEGDMA fraction). This hypothesis seems consistent with the lower zeta potential of the particles crosslinked with 90 equivalents of DEGDMA (-42.8±6.9 mV, *vs.* -56.0±3.7 for those crosslinked with 15 equivalents of DEGDMA, see Table S1), even though this zeta potential difference should be taken with extreme care, given the high standard deviations.

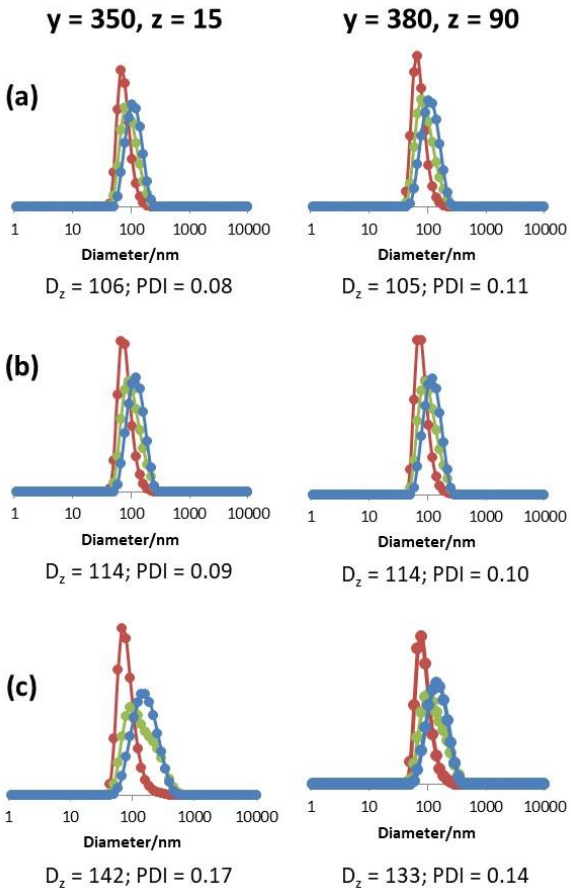

Figure 3. DLS study of core swelling for selected R_0-(SS^-Na^+)$_{140}$-*b*-St_y-*b*-$DEGDMA_z$-SC(S)S*n*Pr CCMs. The measurements were made on filtered solutions (0.45 µm pore filter). (a) Unswollen latex. (b) Swollen by toluene. (c) Swollen by chloroform.

For an equivalent hydrophobic PSt block length, the particle size of the anionic-shell CCMs is similar to that of the neutral particles (*e.g.* D_z(nm)/PDI = 79/0.18 for R_0-(MAA$_{0.5}$-*co*-PEOMA$_{0.5}$)$_{30}$-*b*-(DPPS$_{0.1}$-*co*-St$_{0.9}$)$_{300}$-*b*-(DEGDMA$_{0.1}$-*co*-St$_{0.9}$)$_{100}$-SC(S)S*n*Pr; DPPS = 4-diphenylphosphino-styrene)[24] and of the cationic ones (*e.g.* D_z(nm)/PDI = 109.6/0.04 for R_0-(4VPMe$^+$I$^-$)$_{140}$-*b*-St$_{350}$-*b*-DEGDMA$_{15}$-SC(S)S*n*Pr).[32] Core-swelling experiments were carried out on the two most homogeneous samples *b* and *c*, using toluene and chloroform, both of which are good solvents for polystyrene, using DLS to assess the particle size increase. The results of these experiments (Figure 3) show that chloroform has greater swelling capacity than toluene (the swelling ratios, $D_{z,swollen}/D_{z,unswollen}$, for samples *b* and *c* are 1.340 and 1.267 in $CHCl_3$; 1.075 and 1.086 in toluene; respectively). These swelling abilities are again similar to those previously observed for the neutral- and cationic-shell analogues.[24, 32]

3.5. Completeness of the crosslinking step

A determination of whether the CCM product contains residual uncrosslinked arms is not simple because any free arm would remain entrapped in the CCM particles by self-assembly and would thus remain undetected by DLS and TEM. In addition, free arms and crosslinked polymers are indistinguishable by NMR spectroscopy. The separation of any residual uncrosslinked arms from the crosslinked particles is only possible by dispersion in a medium with good solvent properties for both core and shell. The presence of free diblock chains can then be assessed by an investigation of size-dependent properties such as diffusion (DOSY NMR) or light scattering (DLS). We opted to use the DLS methodology.

The first task was to find a suitable solvent or solvent combination. The hydrophilic P(SS$^-$Na$^+$) block is well-solvated by water but not sufficiently well by neat THF and DMF, which are good solvents for the PSt block. Indeed, the R_0-(SS$^-$Na$^+$)$_x$-SC(S)S*n*Pr macroRAFT intermediates are insoluble in these solvents. The PSt block compatibility with THF and DMF was verified by a DLS study of a R_0-St$_{300}$-SC(S)S*n*Pr homopolymer, made by the ACPA-initiated RAFT polymerization of styrene in water (suspension polymerization) using CTPPA as transfer agent. The as-synthesized

aqueous dispersion contains particles of large dimensions (d ~ 350 nm), but freeze-drying followed by dissolution in THF or DMF gave a narrow distribution of much lower dimensions (d ~ 7.5 or 6.5 nm) indicating the presence of single chains (see Figure S15). Acetone gave aggregates of much larger dimensions (d ~ 300 nm), although in equilibrium with single chains. Therefore, a single solvent for both blocks is not available.

Next, THF/H_2O and DMF/H_2O mixtures were considered and used to investigate the solvation of the diblock R_0-(SS^-Na^+)$_{140}$-*b*-St_{300}-SC(S)S*n*Pr macroRAFT intermediate. The results of the DLS investigations for the R_0-(SS^-Na^+)$_{140}$-*b*-St_{300}-SC(S)S*n*Pr polymer, after freeze-drying and redispersion in THF/H_2O and DMF/H_2O mixtures of various compositions are summarized in Figure S16. These measurements indicate that large agglomerates are present in the neat organic solvent and when the water content is < 40%. However, mixtures containing 40% or more water, both with THF or DMF as cosolvent, yielded single chains as the largely dominating distribution. The size of the distribution is larger in THF/H_2O (d ~ 3-10 nm depending on the composition, the maximum corresponding to the 60/40 composition) than in DMF/H_2O (1.5-3 nm). The best solvent combination to solvate the R_0-(SS^-Na^+)$_{140}$-*b*-St_{300}-SC(S)S*n*Pr single chains thus appears to be the THF/H_2O 60:40 mixture, which was therefore selected for the subsequent investigations of the CCM latexes.

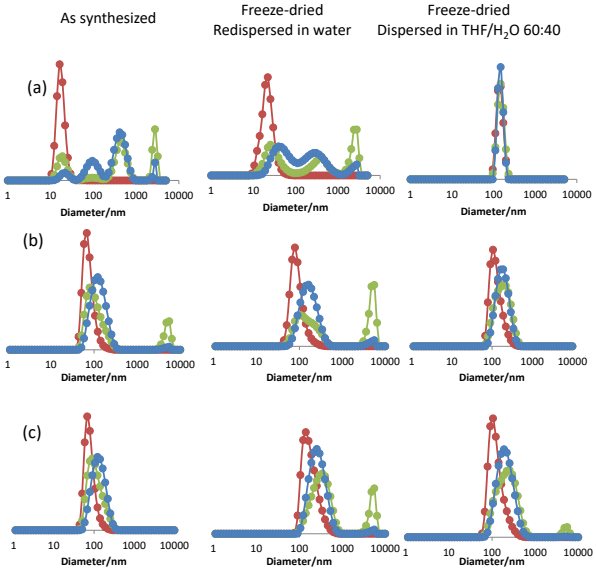

Figure 4. Comparison of the DLS in water and THF/H_2O (60:40) for the R_0-(SS^-Na^+)$_x$-*b*-St_y-*b*-($DEGDMA_z$-*co*-St_w)-SC(S)S*n*Pr CCMs polymers: (a) x = 140, y = 350, z = 15, w = 135; (b) x = 140, y = 350, z = 15, w = 0; (c) x = 140, y = 380, z = 90, w = 0. The dispersions of the freeze-dried samples

were sonicated for 15 min prior to dilution and measurement; all samples were measured from unfiltered solutions. D_z/nm (PDI) values for the dispersions in THF/H_2O 60:40: 241 (0.42) for (a); 170 (0.12) for (b); 188 (0.17) for (c).

These investigations were carried out for the two better-controlled latexes with a neat DEGDMA core crosslinking, R_0-(SS^-Na^+)$_{140}$-*b*-St_y-*b*-$DEGDMA_z$-SC(S)S*n*Pr (y,z = 350,15; 380,90), but also for one of the latexes with a mixed P(DEGDMA-*co*-St) nanogel core. All latexes were freeze-dried and redispersed both in pure water and in the THF/H_2O 60:40 mixture. The results (Figure 4) clearly indicate the absence of detectable populations of single chains. The distributions in THF/H_2O also show the disappearance (or the significant decrease) of the larger-size agglomerates, confirming the nature of the CCM products as single particles with controlled size, which in turn confirms the controlled nature of the chain extension of the hydrosoluble macroRAFT intermediate and of the crosslinking steps. The occasional observation of higher size populations (clearly evident in the volume and intensity modes and not in the number mode) must therefore be ascribed to metastable aggregates that are dissociated in the better-solvating THF/H_2O mixture.

4. Conclusions

In this contribution, we have described the optimized synthesis of well-defined core-crosslinked micelles with a spherical morphology, a polystyrene core and a sodium poly(styrene sulfonate) shell. The PSS^-Na^+-*b*-PSt diblock intermediate forms rather conformationally unstable micelles in water, with facile equilibration with free arms and larger aggregates, but crosslinking produces CCMs with narrow size distribution provided the PS chains are long (> 300 monomer units). Using an optimized 60:40 THF/H_2O mixed solvent as a compatibilizing medium allowed us to establish that the crosslinking step is quantitative (no residual uncrosslinked arm). Equivalent polymers with a ligand-functionalized core for applications in aqueous biphasic catalysis are now being developed and will be reported in a forthcoming contribution.

CRediT authorship contribution statement

Hui Wang: Methodology, Formal analysis, Investigation, Writing – Review & Editing. **Christophe Fliedel**; Supervision, Validation, Writing – Review & Editing. **Eric Manoury**: Project administration, Resources, Writing – Review & Editing. **Rinaldo Poli**: Funding acquisition, Writing – Original Draft, Data curation.

Declaration of competing interest

The authors declare that they have no known competing financial interests or personal relationships that could have appeared to influence the work reported in this paper.

Acknowledgement

We are grateful to the Centre National de la Recherche Scientifique (CNRS) for financial support. We are also grateful to the China Scholarship Council for a Ph.D. fellowship to HW. We thank Lorenzo Vendrame and Dr. Florence Gayet for exploratory investigations.

References

1. Cotanda, P.; Petzetakis, N.; O'Reilly, R. K. Catalytic polymeric nanoreactors: more than a solid supported catalyst. *MRS Communications* **2012,** 2 (4), 119-126.
2. Lu, A.; O'Reilly, R. K. Advances in nanoreactor technology using polymeric nanostructures. *Curr. Opin. Biotech.* **2013,** 24 (4), 639-645 DOI: 10.1016/j.copbio.2012.11.013.
3. Li, Y.; Xiao, K.; Zhu, W.; Deng, W.; Lam, K. S. Stimuli-responsive cross-linked micelles for on-demand drug delivery against cancers. *Advanced Drug Delivery Reviews* **2014,** 66, 58-73 DOI: 10.1016/j.addr.2013.09.008.
4. Talelli, M.; Barz, M.; Rijcken, C. J. F.; Kiessling, F.; Hennink, W. E.; Lammers, T. Core-crosslinked polymeric micelles: Principles, preparation, biomedical applications and clinical translation. *Nano Today* **2015,** 10 (1), 93-117 DOI: 10.1016/j.nantod.2015.01.005.
5. Zhao, Y. Surface-Cross-Linked Micelles as Multifunctionalized Organic Nanoparticles for Controlled Release, Light Harvesting, and Catalysis. *Langmuir* **2016,** 32 (23), 5703-5713 DOI: 10.1021/acs.langmuir.6b01162.
6. Ramasamy, T.; Ruttala, H. B.; Gupta, B.; Poudel, B. K.; Choi, H.-G.; Yong, C. S.; Kim, J. O. Smart chemistry-based nanosized drug delivery systems for systemic applications: A comprehensive review. *Journal of Controlled Release* **2017,** 258, 226-253 DOI: 10.1016/j.jconrel.2017.04.043.
7. Zhang, Y.; Sun, T.; Jiang, C. Biomacromolecules as carriers in drug delivery and tissue engineering. *Acta Pharmaceutica Sinica B* **2018,** 8 (1), 34-50 DOI: 10.1016/j.apsb.2017.11.005.
8. Qu, P.; Kuepfert, M.; Ahmed, E.; Liu, F.; Weck, M. Cross-Linked Polymeric Micelles as Catalytic Nanoreactors. *Eur. J. Inorg. Chem.* **2021,** (15), 1420-1427 DOI: 10.1002/ejic.202100013.
9. Moad, G.; Rizzardo, E.; Thang, S. H. Living radical polymerization by the RAFT process. *Austr. J. Chem.* **2005,** 58 (6), 379-410 DOI: 10.1071/ch05072.

10. Moad, G. RAFT polymerization to form stimuli-responsive polymers. *Polym. Chem.* **2017,** 8 (1), 177-219 DOI: 10.1039/c6py01849a.
11. Charleux, B.; Delaittre, G.; Rieger, J.; D'Agosto, F. Polymerization-Induced Self-Assembly: From Soluble Macromolecules to Block Copolymer Nano-Objects in One Step. *Macromolecules* **2012,** 45 (17), 6753-6765.
12. Warren, N. J.; Armes, S. P. Polymerization-Induced Self-Assembly of Block Copolymer Nano-objects via RAFT Aqueous Dispersion Polymerization. *J. Am. Chem. Soc.* **2014,** 136 (29), 10174-10185.
13. Canning, S. L.; Smith, G. N.; Armes, S. P. A Critical Appraisal of RAFT-Mediated Polymerization-Induced Self Assembly. *Macromolecules* **2016,** 49 (6), 1985-2001 DOI: 10.1021/acs.macromol.5b02602.
14. Penfold, N. J. W.; Yeow, J.; Boyer, C.; Armes, S. P. Emerging Trends in Polymerization-Induced Self-Assembly. *ACS Macro Lett.* **2019,** 8 (8), 1029-1054 DOI: 10.1021/acsmacrolett.9b00464.
15. D'Agosto, F.; Rieger, J.; Lansalot, M. RAFT‐mediated polymerization‐induced self‐assembly. *Angew. Chem. Int. Ed.* **2020,** 59 (22), 8368-8392 DOI: 10.1002/anie.201911758.
16. Sugihara, S.; Armes, S. P.; Blanazs, A.; Lewis, A. L. Non-spherical morphologies from cross-linked biomimetic diblock copolymers using RAFT aqueous dispersion polymerization. *Soft Matter* **2011,** 7 (22), 10787-10793 DOI: 10.1039/c1sm06593a.
17. Chambon, P.; Blanazs, A.; Battaglia, G.; Armes, S. P. How Does Cross-Linking Affect the Stability of Block Copolymer Vesicles in the Presence of Surfactant? *Langmuir* **2012,** 28 (2), 1196-1205 DOI: 10.1021/la204539c.
18. Zhou, W.; Qu, Q. W.; Yu, W. J.; An, Z. S. Single Monomer for Multiple Tasks: Polymerization Induced Self-Assembly, Functionalization and Cross-Linking, and Nanoparticle Loading. *ACS Macro Lett.* **2014,** 3 (12), 1220-1224 DOI: 10.1021/mz500650c.
19. Figg, C. A.; Simula, A.; Gebre, K. A.; Tucker, B. S.; Haddleton, D. M.; Sumerlin, B. S. Polymerization-induced thermal self-assembly (PITSA). *Chem. Sci.* **2015,** 6 (2), 1230-1236 DOI: 10.1039/c4sc03334e.
20. Qu, Q. W.; Liu, G. Y.; Lv, X. Q.; Zhang, B. H.; An, Z. S. In Situ Cross-Linking of Vesicles in Polymerization-Induced Self Assembly. *ACS Macro Lett.* **2016,** 5 (3), 316-320 DOI: 10.1021/acsmacrolett.6b00066.
21. Chambon, P.; Blanazs, A.; Battaglia, G.; Armes, S. P. Facile Synthesis of Methacrylic ABC Triblock Copolymer Vesicles by RAFT Aqueous Dispersion Polymerization. *Macromolecules* **2012,** 45 (12), 5081-5090 DOI: 10.1021/ma300816m.
22. Cao, J. P.; Tan, Y. X.; Dai, X. C.; Chen, Y.; Zhang, L.; Tan, J. B. In situ cross-linking in RAFT-mediated emulsion polymerization: Reshaping the preparation of cross-linked block copolymer nano-objects by polymerization-induced self-assembly. *Polymer* **2021,** 230, DOI: 10.1016/j.polymer.2021.124095.
23. Damsongsang, P.; Hoven, V. P.; Yusa, S. I. Core-functionalized nanoaggregates: preparation via polymerization-induced self-assembly and their applications. *New J. Chem.* **2021,** 45 (29), 12776-12791 DOI: 10.1039/d1nj01791h.
24. Zhang, X.; Cardozo, A. F.; Chen, S.; Zhang, W.; Julcour, C.; Lansalot, M.; Blanco, J.-F.; Gayet, F.; Delmas, H.; Charleux, B.; Manoury, E.; D'Agosto, F.; Poli, R. Core-Shell Nanoreactors for Efficient Aqueous Biphasic Catalysis. *Chem. Eur. J.* **2014,** 20 (47), 15505–15517 DOI: 10.1002/chem.201403819.
25. Chen, S.; Cardozo, A. F.; Julcour, C.; Blanco, J.-F.; Barthe, L.; Gayet, F.; Charleux, B.; Lansalot, M.; D'Agosto, F.; Delmas, H.; Manoury, E.; Poli, R. Amphiphilic Core-Cross-linked Micelles functionalized with Bis(4-methoxyphenyl)phenylphosphine as catalytic nanoreactors for biphasic hydroformylation. *Polymer* **2015,** 72, 327-335 DOI: 10.1016/j.polymer.2015.02.024.
26. Joumaa, A.; Gayet, F.; Garcia-Suarez, E. J.; Himmelstrup, J.; Riisager, A.; Poli, R.; Manoury, E. Synthesis of Nixantphos core-functionalized amphiphilic nanoreactors and application

to rhodium-catalyzed aqueous biphasic 1-octene hydroformylation. *Polymers* **2020,** 12, 1107/1-18 DOI: 10.3390/polym12051107.
27. Cardozo, A. F.; Julcour, C.; Barthe, L.; Blanco, J.-F.; Chen, S.; Gayet, F.; Manoury, E.; Zhang, X.; Lansalot, M.; Charleux, B.; D'Agosto, F.; Poli, R.; Delmas, H. Aqueous phase homogeneous catalysis using core-shell nano-reactors: application to rhodium catalyzed hydroformylation of 1-octene. *J. Catal.* **2015,** 324, 1-8 DOI: 10.1016/j.jcat.2015.01.009.
28. Poli, R.; Chen, S.; Zhang, X.; Cardozo, A.; Lansalot, M.; D'Agosto, F.; Charleux, B.; Manoury, E.; Gayet, F.; Julcour, C.; Blanco, J.-F.; Barthe, L.; Delmas, H. One-Pot RAFT Synthesis of Triphenylphosphine-Functionalized Amphiphilic Core-Shell Polymers and Application as Catalytic Nanoreactors in Aqueous Biphasic Hydroformylation. *ACS Symp. Ser.* **2015,** 1188, 203-220.
29. Lobry, E.; Cardozo, A. F.; Barthe, L.; Blanco, J.-F.; Delmas, H.; Chen, S.; Gayet, F.; Zhang, X.; Lansalot, M.; D'Agosto, F.; Poli, R.; Manoury, E.; Julcour, C. Core phosphine-functionalized amphiphilic nanogels as catalytic nanoreactors for aqueous biphasic hydroformylation. *J. Catal.* **2016,** 342, 164-172 DOI: 10.1016/j.jcat.2016.07.023.
30. Manoury, E.; Gayet, F.; D'Agosto, F.; Lansalot, M.; Delmas, H.; Julcour, C.; Blanco, J.-F.; Barthe, L.; Poli, R., Core-cross-linked micelles and amphiphilic nanogels as unimolecular nanoreactors for micellar-type, metal-based aqueous biphasic catalysis. In *Effects of Nanoconfinement on Catalysis*, Poli, R., Ed. Springer: New York, 2017; pp 147-172.
31. Joumaa, A.; Chen, S.; Vincendeau, S.; Gayet, F.; Poli, R.; Manoury, E. Rhodium-catalyzed aqueous biphasic hydrogenation of alkenes with amphiphilic phosphine-containing core-shell polymers. *Mol. Cat.* **2017,** 438, 267-271 DOI: 10.1016/j.mcat.2017.06.005.
32. Wang, H.; Vendrame, L.; Fliedel, C.; Chen, S.; Gayet, F.; Manoury, E.; Zhang, X.; D'Agosto, F.; Lansalot, M.; Poli, R. Core-cross-linked micelles made by RAFT polymerization with a poly-cationic outer shell based on poly(1-methyl-4-vinylpyridinium). *Macromolecules* **2020,** 53 2198-2208 DOI: 10.1021/acs.macromol.9b02582. .
33. Wang, H.; Vendrame, L.; Fliedel, C.; Chen, S.; Gayet, F.; D'Agosto, F.; Lansalot, M.; Manoury, E.; Poli, R. Triphenylphosphine-functionalized core-cross-linked micelles and nanogels with a polycationic outer shell: synthesis and application in rhodium-catalyzed biphasic hydrogenations. *Chem. Eur. J.* **2021,** 27, 5205–5214 DOI: 10.1002/chem.202004689.
34. Wang, H.; Fiore, A. M.; Fliedel, C.; Manoury, E.; Philippot, K.; Dell'Anna, M. M.; Mastrorilli, P.; Poli, R. Rhodium nanoparticles inside well-defined unimolecular amphiphilic polymeric nanoreactors: synthesis and biphasic hydrogenation catalysis. *Nanoscale Advances* **2021,** 3, 2554-2566 DOI: 10.1039/D1NA00028D.
35. Semsarilar, M.; Ladmiral, V.; Blanazs, A.; Armes, S. P. Anionic Polyelectrolyte-Stabilized Nanoparticles via RAFT Aqueous Dispersion Polymerization. *Langmuir* **2012,** 28 (1), 914-922 DOI: 10.1021/la203991y.
36. Velasquez, E.; Rieger, J.; Stoffelbach, F.; D'Agosto, F.; Lansalot, M.; Dufils, P.-E.; Vinas, J. Surfactant-free poly(vinylidene chloride) latexes via one-pot RAFT-mediated aqueous polymerization. *Polymer* **2016,** 106, 275-284 DOI: 10.1016/j.polymer.2016.08.083.
37. Tang, B.-k.; Li, J.; Ren, Q.; Wang, C.-y. Synthesis of poly(sodium styrene sulfonate)-b-poly(butyl acrylate) block copolymers via RAFT emulsifier-free emulsion polymerization and their application in PEDOT aqueous dispersions. *Synthetic Metals* **2019,** 258, DOI: 10.1016/j.synthmet.2019.116188.
38. Gurnani, P.; Bray, C. P.; Richardson, R. A. E.; Peltier, R.; Perrier, S. Heparin-Mimicking Sulfonated Polymer Nanoparticles via RAFT Polymerization-Induced Self-Assembly. *Macromol. Rapid Comm.* **2019,** 40 (2), DOI: 10.1002/marc.201800314.
39. Chen, S.; Gayet, F.; Manoury, E.; Joumaa, A.; Lansalot, M.; D'Agosto, F.; Poli, R. Coordination chemistry inside polymeric nanoreactors: interparticle metal exchange processes and ionic compound vectorization in phosphine-functionalized amphiphilic polymer latexes. *Chem. Eur. J.* **2016,** 22, 6302 – 6313 DOI: 10.1002/chem.201504923.

40. Chen, S.; Manoury, E.; Gayet, F.; Poli, R. Coordination chemistry inside polymeric nanoreactors: metal migration and cross-exchange in amphiphilic core-shell polymer latexes. *Polymers* **2016,** 8 (2), 26/1-18 DOI: 10.3390/polym8020026.
41. Boursier, T.; Chaduc, I.; Rieger, J.; D'Agosto, F.; Lansalot, M.; Charleux, B. Controlled radical polymerization of styrene in miniemulsion mediated by PEO-based trithiocarbonate macromolecular RAFT agents. *Polym. Chem.* **2011,** 2 (2), 355-362 DOI: 10.1039/c0py00237b.
42. Yeole, N.; Hundiwale, D. Effect of hydrophilic macro-RAFT agent in surfactant-free emulsion polymerization. *Colloids Surf., A* **2011,** 392 (1), 329-334 DOI: 10.1016/j.colsurfa.2011.10.011.
43. Yeole, N.; Hundiwale, D.; Jana, T. Synthesis of core-shell polystyrene nanoparticles by surfactant free emulsion polymerization using macro-RAFT agent. *Journal of Colloid and Interface Science* **2011,** 354 (2), 506-510 DOI: 10.1016/j.jcis.2010.11.021.
44. Yeole, N.; Hundiwale, D. Effect of varying hydrophobic monomers and their copolymerization in surfactant-free emulsion polymerizations using a macro-RAFT agent. *RSC Adv.* **2013,** 3 (44), 22213-22218 DOI: 10.1039/c3ra44402c.
45. Yeole, N.; Kutcherlapati, S. N. R.; Jana, T. Polystyrene-graphene oxide (GO) nanocomposite synthesized by interfacial interactions between RAFT modified GO and core-shell polymeric nanoparticles. *Journal of Colloid and Interface Science* **2015,** 443, 137-142 DOI: 10.1016/j.jcis.2014.11.071.
46. He, W. D.; Sun, X. L.; Wan, W. M.; Pan, C. Y. Multiple Morphologies of PAA-b-PSt Assemblies throughout RAFT Dispersion Polymerization of Styrene with PAA Macro-CTA. *Macromolecules* **2011,** 44 (9), 3358-3365 DOI: 10.1021/ma2000674.
47. Yang, P. C.; Ratcliffe, L. P. D.; Armes, S. P. Efficient Synthesis of Poly(methacrylic acid)-block-Poly(styrene-alt-N-phenylmaleimide) Diblock Copolymer Lamellae Using RAFT Dispersion Polymerization. *Macromolecules* **2013,** 46 (21), 8545-8556 DOI: 10.1021/ma401797a.
48. Ning, Y.; Fielding, L. A.; Andrews, T. S.; Growney, D. J.; Armes, S. P. Sulfate-based anionic diblock copolymer nanoparticles for efficient occlusion within zinc oxide. *Nanoscale* **2015,** 7 (15), 6691-6702 DOI: 10.1039/c5nr00535c.
49. Hanisch, A.; Yang, P. C.; Kulak, A. N.; Fielding, L. A.; Meldrum, F. C.; Armes, S. P. Phosphonic Acid-Functionalized Diblock Copolymer Nano-Objects via Polymerization-Induced Self-Assembly: Synthesis, Characterization, and Occlusion into Calcite Crystals. *Macromolecules* **2016,** 49 (1), 192-204 DOI: 10.1021/acs.macromol.5b02212.
50. Liu, Y. Q.; Pollock, K. L.; Cavicchi, K. A. Synthesis of poly(trioctylammonium p-styrenesulfonate) homopolymers and block copolymers by RAFT polymerization. *Polymer* **2009,** 50 (26), 6212-6217 DOI: 10.1016/j.polymer.2009.10.069.
51. Fan, Z. Y.; Zhao, Y.; Preda, F.; Clacens, J. M.; Shi, H.; Wang, L. M.; Feng, X. S.; De Campo, F. Preparation of bio-based surfactants from glycerol and dodecanol by direct etherification. *Green Chem.* **2015,** 17 (2), 882-892 DOI: 10.1039/c4gc00818a.